Figure S1

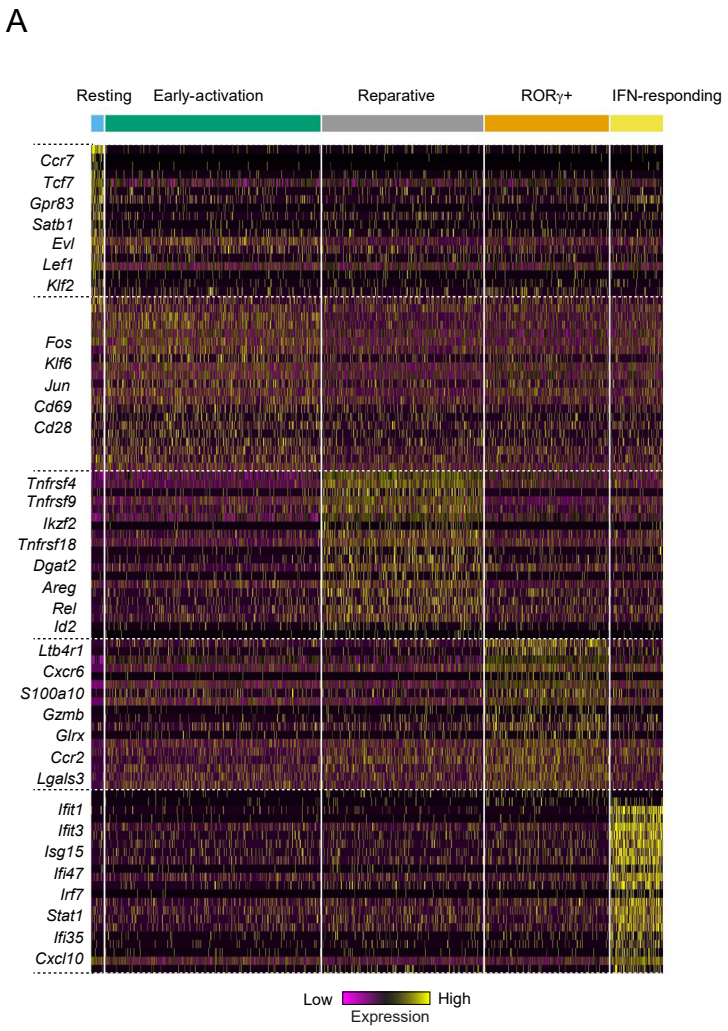
A
Resting
Early-activation
Reparative
RORγ+
IFN-responding
Ccr7
Tcf7
Gpr83
Satb1
Evl
Lef1
Klf2
Fos
Klf6
Jun
Cd69
Cd28
Tnfrsf4
Tnfrsf9
Ikzf2
Tnfrsf18
Dgat2
Areg
Rel
Id2
Ltb4r1
Cxcr6
S100a10
Gzmb
Glrx
Ccr2
Lgals3
Ifit1
Ifit3
Isg15
Ifi47
Irf7
Stat1
Ifi35
Cxcl10
Low
High
Expression

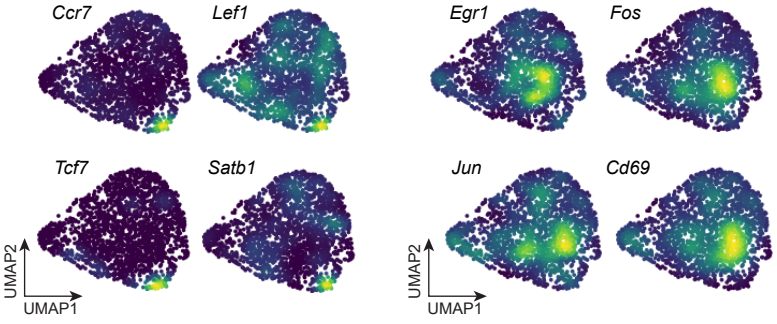
B
Ccr7
Lef1
Tcf7
Satb1
UMAP2
UMAP1
C
Egr1
Fos
Jun
Cd69
UMAP2
UMAP1

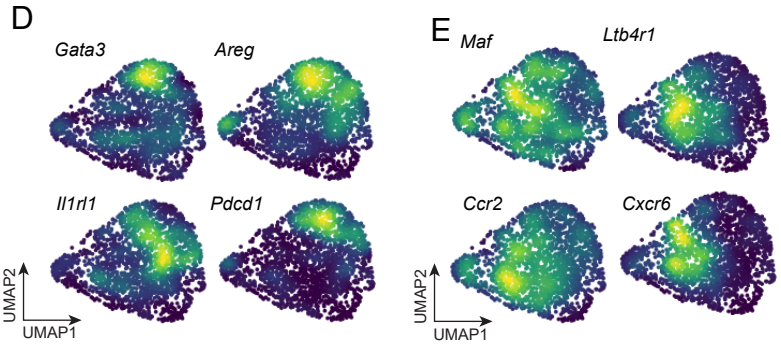
D
Gata3
Areg
Il1rl1
Pdcd1
UMAP2
UMAP1
E
Maf
Ltb4r1
Ccr2
Cxcr6
UMAP2
UMAP1

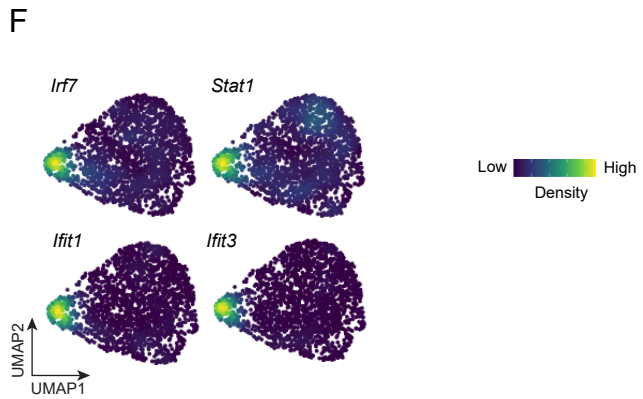
F
Irf7
Stat1
Ifit1
Ifit3
UMAP2
UMAP1
Low
High
Density

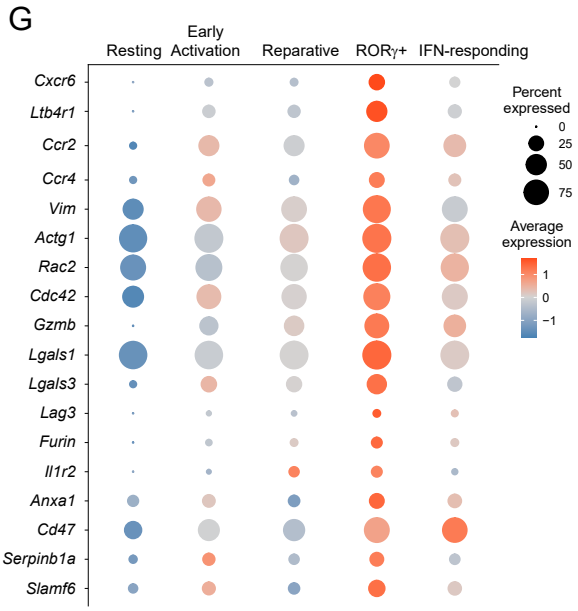
G
Resting
Early Activation
Reparative
RORγ+
IFN-responding
Cxcr6
Ltb4r1
Ccr2
Ccr4
Vim
Actg1
Rac2
Cdc42
Gzmb
Lgals1
Lgals3
Lag3
Furin
Il1r2
Anxa1
Cd47
Serpinb1a
Slamf6
Percent expressed
0
25
50
75
Average expression
1
0
−1

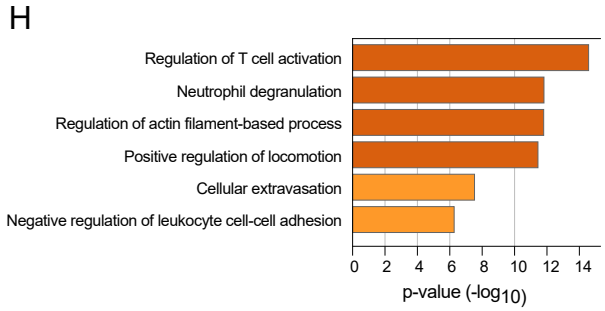
H
Regulation of T cell activation
Neutrophil degranulation
Regulation of actin filament-based process
Positive regulation of locomotion
Cellular extravasation
Negative regulation of leukocyte cell-cell adhesion
0
2
4
6
8
10
12
14
p-value (-log10)

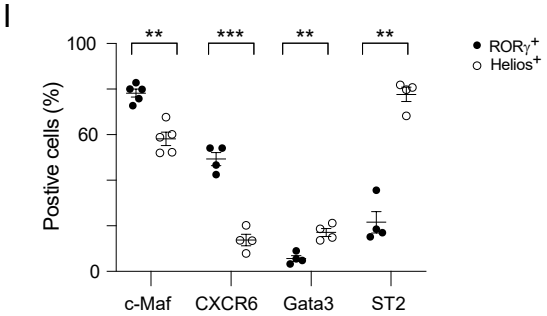
I
100
60
0
Postive cells (%)
**
***
**
**
RORγ+
Helios+
c-Maf
CXCR6
Gata3
ST2

Figure S1 (Related to Figure 1): Characterization of RORγ^{+} Treg cells in skeletal muscle after acute injury

(A-H) scRNA-seq of Treg cells from hindlimb muscles of *Foxp3^{GFP}* mice 3 days after CTX-induced injury. A) Heatmap of the top 20 differentially expressed genes in each cluster *vis-à-vis* all other clusters. B) Resting, C) early-activation, D) reparative, E) RORγ^{+} and F) IFN-responding Treg clusters' expression of key marker genes shown as density plots. G) Bubble-plot of the average transcript expression of key RORγ^{+} Treg cell marker genes. H) Pathway analysis of up-regulated transcripts in the RORγ^{+} Treg subtype relative to other subtypes. (I) Flow-cytometry of c-Maf, CXCR6, Gata3 and ST2 expression in RORγ^{+} and Helios^{+} muscle Treg cells 3 days after CTX injury. Unpaired t-test (I).

Figure S2

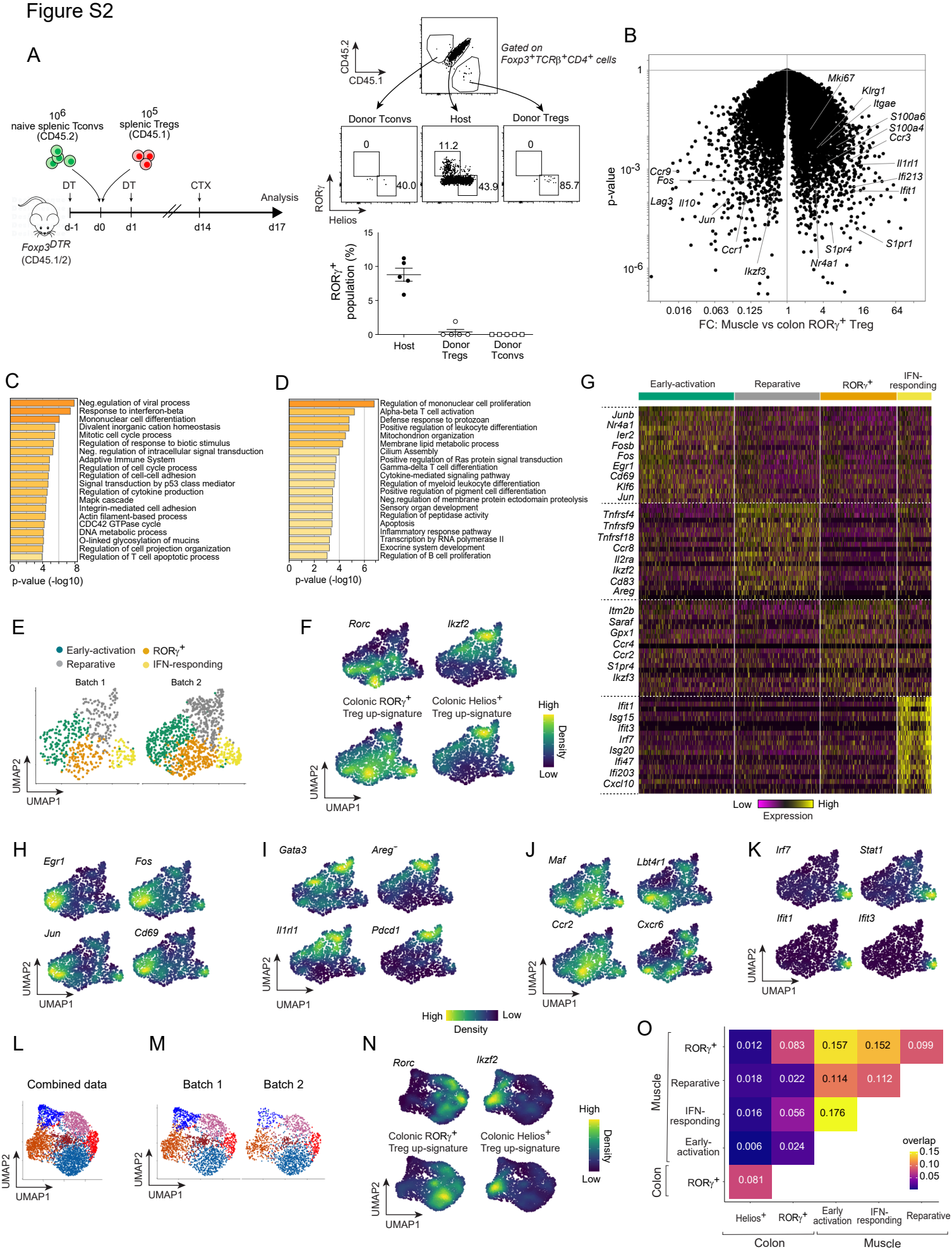
A
10^6 naive splenic Tconvs (CD45.2)
10^5 splenic Tregs (CD45.1)
DT
DT
CTX
Analysis
d-1
d0
d1
d14
d17
Foxp3^DTR (CD45.1/2)
CD45.2
CD45.1
Gated on Foxp3+TCRβ+CD4+ cells
Donor Tconvs
Host
Donor Tregs
0
40.0
11.2
43.9
0
85.7
RORγ
Helios
RORγ+ population (%)
Host
Donor Tregs
Donor Tconvs
B
p-value
FC: Muscle vs colon RORγ+ Treg
Mki67
Klrg1
Itgae
S100a6
S100a4
Ccr3
Il1rl1
Ifi213
Ifit1
S1pr1
S1pr4
Nr4a1
Ikzf3
Ccr1
Jun
Il10
Lag3
Fos
Ccr9
C
Neg.egulation of viral process
Response to interferon-beta
Mononuclear cell differentiation
Divalent inorganic cation homeostasis
Mitotic cell cycle process
Regulation of response to biotic stimulus
Neg. regulation of intracellular signal transduction
Adaptive Immune System
Regulation of cell cycle process
Regulation of cell-cell adhesion
Signal transduction by p53 class mediator
Regulation of cytokine production
Mapk cascade
Integrin-mediated cell adhesion
Actin filament-based process
CDC42 GTPase cycle
DNA metabolic process
O-linked glycosylation of mucins
Regulation of cell projection organization
Regulation of T cell apoptotic process
p-value (-log10)
D
Regulation of mononuclear cell proliferation
Alpha-beta T cell activation
Defense response to protozoan
Positive regulation of leukocyte differentiation
Mitochondrion organization
Membrane lipid metabolic process
Cilium Assembly
Positive regulation of Ras protein signal transduction
Gamma-delta T cell differentiation
Cytokine-mediated signaling pathway
Regulation of myeloid leukocyte differentiation
Positive regulation of pigment cell differentiation
Neg.regulation of membrane protein ectodomain proteolysis
Sensory organ development
Regulation of peptidase activity
Apoptosis
Inflammatory response pathway
Transcription by RNA polymerase II
Exocrine system development
Regulation of B cell proliferation
p-value (-log10)
G
Early-activation
Reparative
RORγ+
IFN-responding
Junb
Nr4a1
Ier2
Fosb
Fos
Egr1
Cd69
Klf6
Jun
Tnfrsf4
Tnfrsf9
Tnfrsf18
Ccr8
Il2ra
Ikzf2
Cd83
Areg
Itm2b
Saraf
Gpx1
Ccr4
Ccr2
S1pr4
Ikzf3
Ifit1
Isg15
Ifit3
Irf7
Isg20
Ifi47
Ifi203
Cxcl10
Low
High
Expression
E
Early-activation
RORγ+
Reparative
IFN-responding
Batch 1
Batch 2
UMAP2
UMAP1
F
Rorc
Ikzf2
Colonic RORγ+ Treg up-signature
Colonic Helios+ Treg up-signature
High
Density
Low
UMAP2
UMAP1
H
Egr1
Fos
Jun
Cd69
UMAP2
UMAP1
I
Gata3
Areg−
Il1rl1
Pdcd1
UMAP2
UMAP1
High
Low
Density
J
Maf
Lbt4r1
Ccr2
Cxcr6
UMAP2
UMAP1
K
Irf7
Stat1
Ifit1
Ifit3
UMAP2
UMAP1
L
Combined data
UMAP2
UMAP1
M
Batch 1
Batch 2
UMAP2
UMAP1
N
Rorc
Ikzf2
Colonic RORγ+ Treg up-signature
Colonic Helios+ Treg up-signature
High
Density
Low
UMAP2
UMAP1
O
Muscle
Colon
RORγ+
Reparative
IFN-responding
Early-activation
RORγ+
0.012
0.083
0.157
0.152
0.099
0.018
0.022
0.114
0.112
0.016
0.056
0.176
0.006
0.024
0.081
overlap
0.15
0.10
0.05
Helios+
RORγ+
Early activation
IFN-responding
Reparative
Colon
Muscle

Figure S2 (Related to Figure 2): Relationship between muscle and colon RORγ⁺ Treg cells

(A) Congenically labelled naïve Tconv or Treg cells were sorted from spleen and transferred into Treg-depleted *Foxp3*^{DTR} mice followed by CTX-induced injury. Experimental design (left), representative dot-plots (top right) and summary data (bottom right) of RORγ⁺ fraction within muscle Foxp3⁺ cells originating from each donor pool. (B-D) *Foxp3*$^{Thy1.1}$x *Rorc*$^{GFP/wt}$ male mice were injected with CTX. After 3 day, RORγ⁺ Treg cells (CD4⁺TCRβ⁺Foxp3$^{Thy1.1+}$RORγ^{GFP+}) were sorted from muscle and colon, and their transcriptional profiles were determined using population-level RNA-seq. B) Volcano plot illustrating FC differences between the two populations. C) Pathway analysis of up-regulated transcripts in muscle, and D) colon RORγ⁺ Treg cells. (E-O) Paired scRNA-seq and sc*Tcr*-seq of muscle (E-K) or colon (L-N) Treg cells from 6 individual *Foxp3*^{GFP} mice on day 3 after CTX injection. E) 2D UMAP plot of muscle Treg cells illustrating the distribution of cells from two experimental batches. F) Density plot of the indicated genes and signatures. G) Heatmap of the top 20 differentially expressed genes in each cluster. H) Early-activation, I) reparative, J) RORγ⁺ and K) IFN-responding Treg clusters' expression of key marker genes shown as density plots. L) 2D UMAP plot of colon Treg cells; and M) cell distribution across two experimental batches. N) Density plot of *Rorc, Ikzf2,* and the colonic RORγ⁺ or Helios⁺ Treg up-signatures. O) Heatmap of the clonal overlap score between different muscle and colon Treg subtypes.

Figure S3

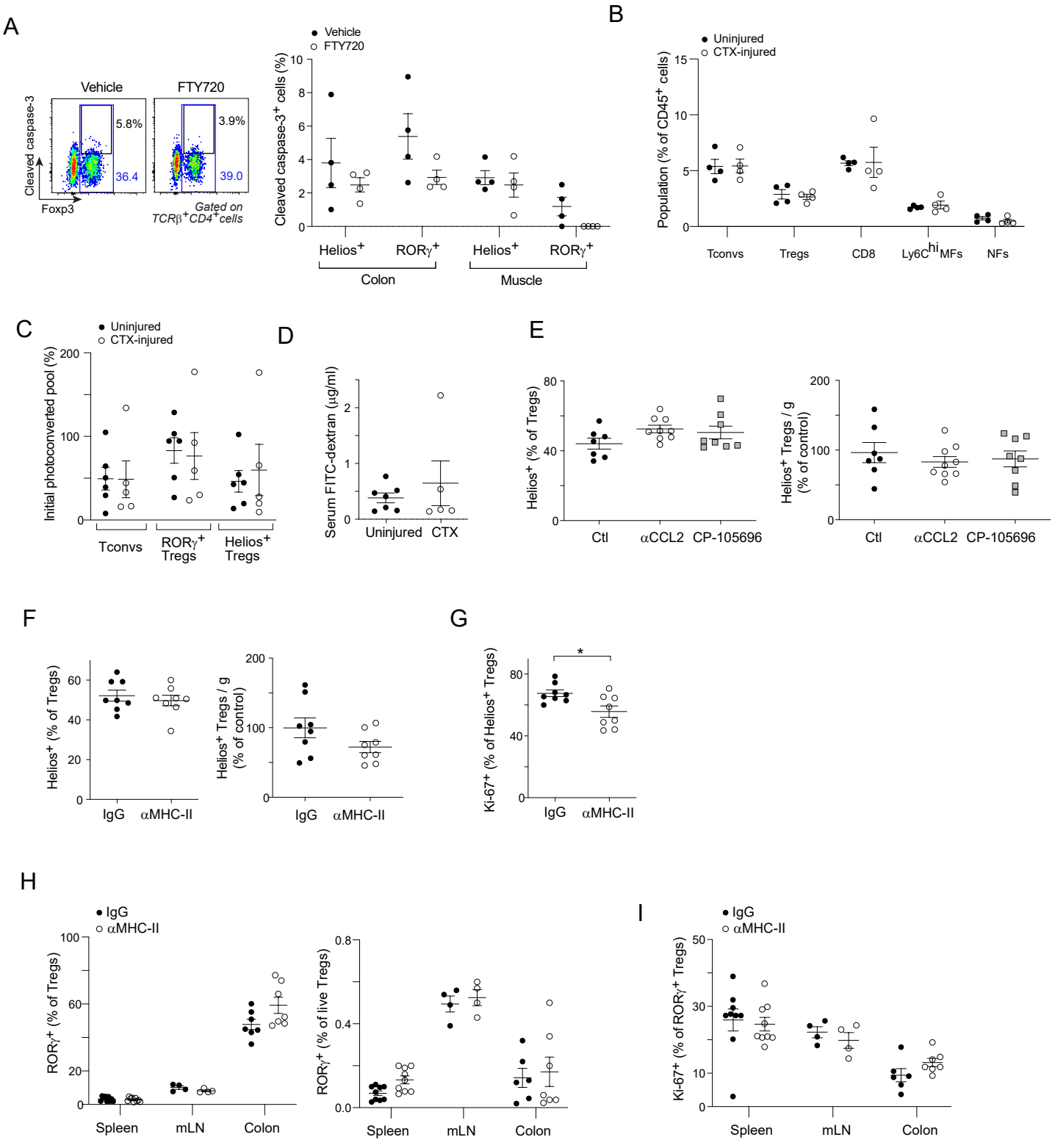
A
Vehicle
FTY720
Cleaved caspase-3
5.8%
36.4
3.9%
39.0
Foxp3
Gated on TCRβ+CD4+cells
Vehicle
FTY720
Cleaved caspase-3+ cells (%)
Helios+
RORγ+
Helios+
RORγ+
Colon
Muscle
B
Uninjured
CTX-injured
Population (% of CD45+ cells)
Tconvs
Tregs
CD8
Ly6Chi MFs
NFs
C
Uninjured
CTX-injured
Initial photoconverted pool (%)
Tconvs
RORγ+ Tregs
Helios+ Tregs
D
Serum FITC-dextran (μg/ml)
Uninjured
CTX
E
Helios+ (% of Tregs)
Ctl
αCCL2
CP-105696
Helios+ Tregs / g (% of control)
Ctl
αCCL2
CP-105696
F
Helios+ (% of Tregs)
IgG
αMHC-II
Helios+ Tregs / g (% of control)
IgG
αMHC-II
G
Ki-67+ (% of Helios+ Tregs)
*
IgG
αMHC-II
H
IgG
αMHC-II
RORγ+ (% of Tregs)
Spleen
mLN
Colon
RORγ+ (% of live Tregs)
Spleen
mLN
Colon
I
IgG
αMHC-II
Ki-67+ (% of RORγ+ Tregs)
Spleen
mLN
Colon

Figure S3 (Related to Figure 3): Mechanisms of RORγ$^+$ Treg accumulation in regenerating muscle

(A) Flow-cytometric quantification of cleaved caspase-3 in colon and muscle Helios$^+$ and RORγ$^+$ Treg cells after 1 day of CTX-induced injury in vehicle- or FTY720-treated mice. Representative dot-plots (middle, one experiment) and summary data. (B) Flow-cytometric quantification of the indicated immunocyte compartments in the colon of uninjured or 3 day-injured mice. (C) The descending colon of Kaede mice was photoconverted (PhC) and hindlimb muscle were injected or not with CTX. Flow-cytometric quantification of egress of diverse lymphocyte populations from the colon after 24 hr in uninjured and CTX-injured mice. (D) Intestinal permeability, as measured by FITC-dextran concentrations in the serum, in uninjured or 3-day injured mice. (E) Flow-cytometric quantification of Helios$^+$ Treg cell fraction (left) and number (right) in hindlimb muscles 2 days after CTX-induced injury in control- (Ctl), αCCL2-, or CP-105696-treated mice. (F-I) Mice were treated with isotype (IgG) or anti-mouse MHC Class II (I-A/I-E) antibody (αMHC-II), and flow-cytometric quantification was performed 3 days after CTX injury. F) Muscle Helios$^+$ Treg cell fraction (left) and number (right). G) Ki-67$^+$ fraction in muscle Helios$^+$ Treg cells. H) RORγ$^+$ Treg cell fraction, and G) Ki-67$^+$ fraction in RORγ$^+$ Treg cells from diverse organs. Unpaired t-test (G). MFs: macrophages; NFs: neutrophils; mLN: mesenteric lymph nodes.

Figure S4

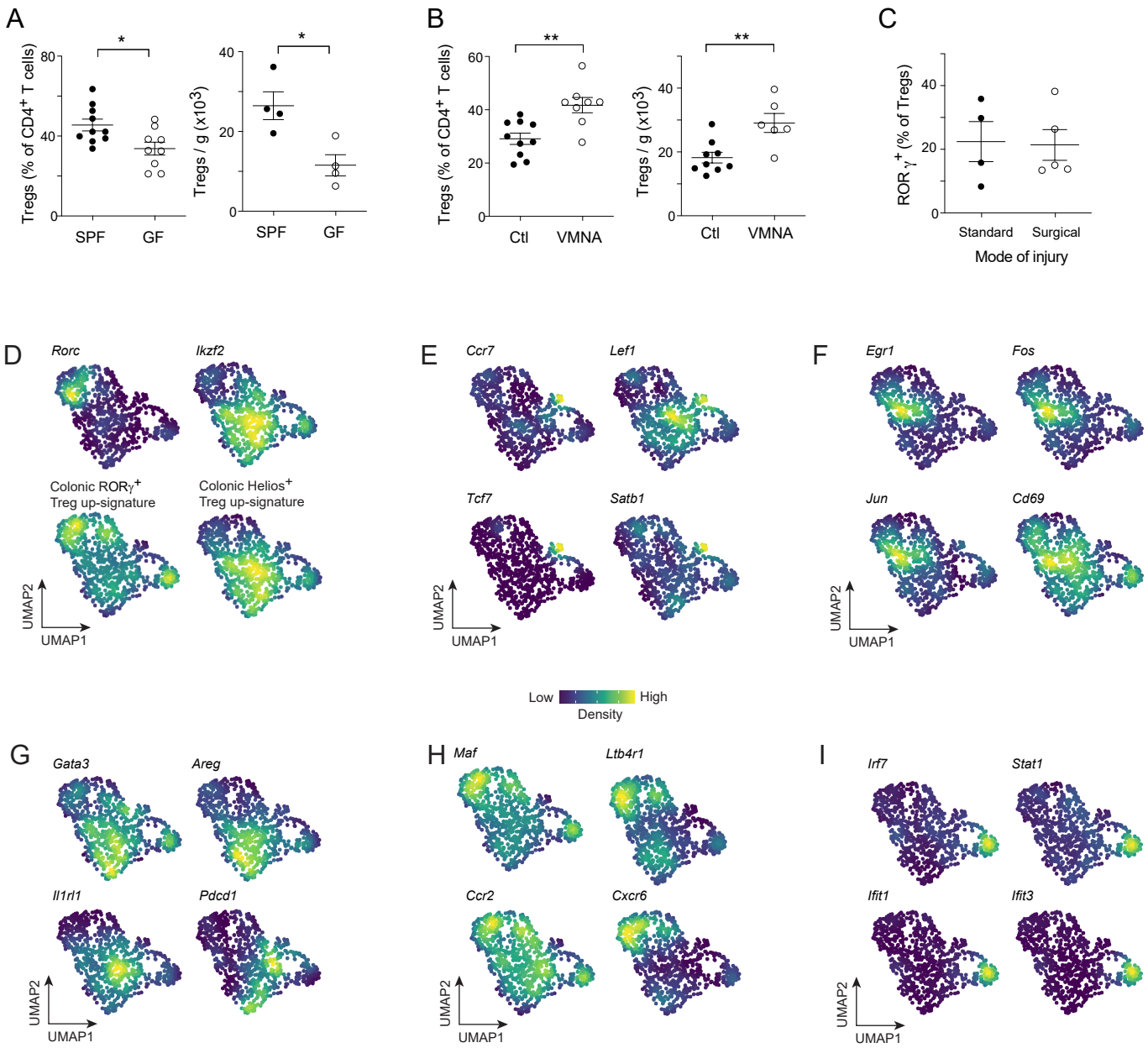

Figure S4 (Related to Figure 4): Microbiota impacts on muscle Treg cells after acute injury

(A) Flow-cytometric quantification of total Treg cell fraction (left) and number (right) in hindlimb muscle 3 days after CTX-induced injury of specific-pathogen-free (SPF) or germ-free (GF) mice. (B) Same as A except SPF mice were treated or not with the antibiotic cocktail, VMNA (vancomycin, metronidazole, neomycin, ampicillin). (C) Flow-cytometric quantification of muscle RORγ⁺ Treg cells 3 days after standard or sterile surgical CTX-induced injury. (D-I) scRNA-seq comparison of muscle Treg cells from vehicle- and VMNA-treated *Foxp3*^{GFP} mice 3 days after CTX injury. D) Density plot of *Rorc*, *Ikzf2,* the colonic RORγ⁺, and Helios⁺ Treg up-signatures. E) Resting, F) early-activation, G) reparative, H) RORγ⁺, and I) IFN-responding Treg clusters' expression of key marker genes shown as density plots. Unpaired t-test (A, B).

Figure S5

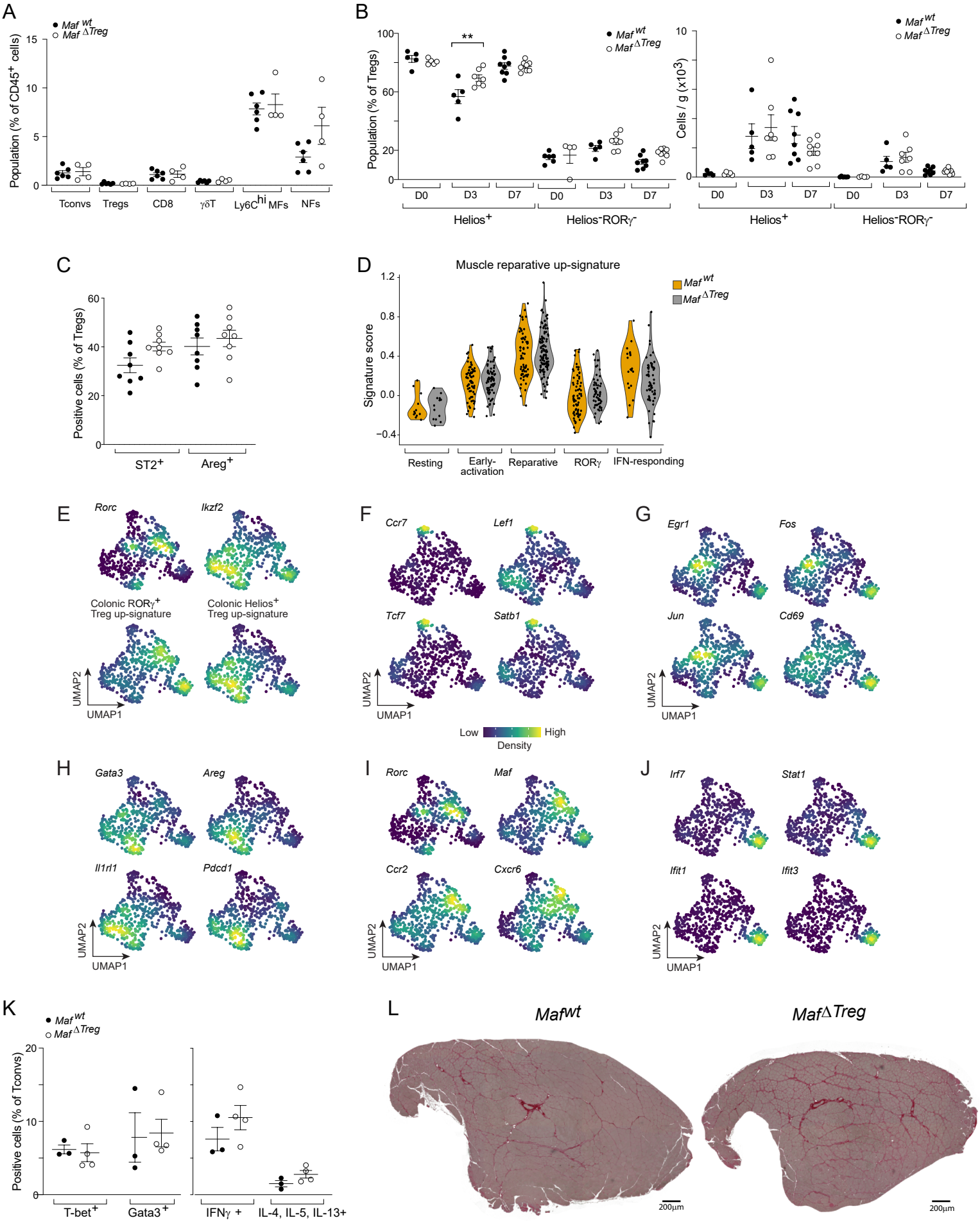
A
Maf wt
Maf ΔTreg
Population (% of CD45+ cells)
Tconvs
Tregs
CD8
γδT
Ly6C hi MFs
NFs
B
Population (% of Tregs)
Cells / g (x10^3)
**
D0
D3
D7
Helios+
Helios-RORγ-
C
Positive cells (% of Tregs)
ST2+
Areg+
D
Muscle reparative up-signature
Signature score
Resting
Early-activation
Reparative
RORγ
IFN-responding
E
Rorc
Ikzf2
Colonic RORγ+ Treg up-signature
Colonic Helios+ Treg up-signature
UMAP1
UMAP2
F
Ccr7
Lef1
Tcf7
Satb1
Low
High
Density
G
Egr1
Fos
Jun
Cd69
H
Gata3
Areg
Il1rl1
Pdcd1
I
Rorc
Maf
Ccr2
Cxcr6
J
Irf7
Stat1
Ifit1
Ifit3
K
Positive cells (% of Tconvs)
T-bet+
Gata3+
IFNγ +
IL-4, IL-5, IL-13+
L
Mafwt
MafΔTreg
200μm

Figure S5 (Related to Figure 5): Regulation of muscle inflammation and fibrosis by RORγ$^+$ Treg cells

Comparisons of hindlimb muscles from *Maf*^{wt} and *Maf*$^{\Delta Treg}$ littermates 0, 3 or 7 days after CTX-induced injury. (A) Flow-cytometric quantification of the indicated immunocyte compartments in muscle at steady-state. (B) Flow-cytometric quantification of the fraction (left) and number (right) of muscle Helios$^+$ and Helios$^-$ RORγ$^-$ Treg cells. (C) Flow-cytometric quantification of ST2 and Areg in muscle Treg cells 7 days after CTX-induced injury. (D-J) scRNA-seq comparison of muscle Treg cells from *Maf*^{wt} and *Maf*$^{\Delta Treg}$ mice 3 days after CTX-induced injury. D) Violin plot of the expression of muscle reparative Treg up-signature genes across different Treg subtypes in the two genotypes. E) Density plot of *Rorc*, *Ikzf2,* colonic RORγ$^+$, and Helios$^+$ Treg up-signatures. F) Resting, G) early-activation, H) reparative, I) RORγ$^+$ and J) IFN-responding Treg clusters' expression of key marker genes shown as density plots. (K) Flow-cytometric quantification of T-bet$^+$ and Gata3$^+$ (left), and (PMA+ionomycin)-stimulated production of IFNγ and IL-4+IL-5+IL-13 by muscle Tconv cells 3 days after CTX injury. (L) Representative images of picrosirius red staining 7 days after CTX injury (4 independent experiments). Two-way ANOVA (B).

Figure S6

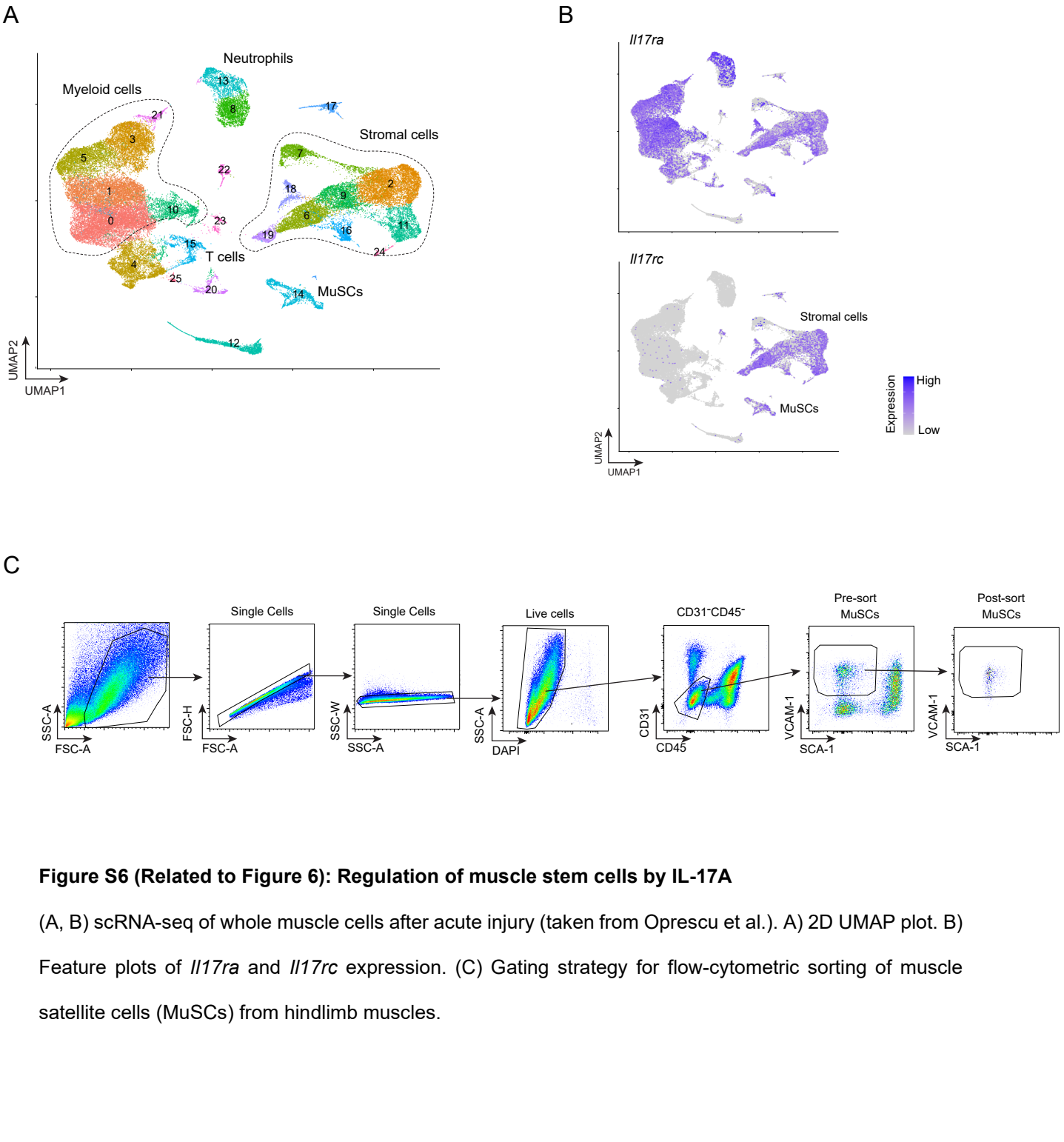

Figure S6 (Related to Figure 6): Regulation of muscle stem cells by IL-17A

(A, B) scRNA-seq of whole muscle cells after acute injury (taken from Oprescu et al.). A) 2D UMAP plot. B) Feature plots of *Il17ra* and *Il17rc* expression. (C) Gating strategy for flow-cytometric sorting of muscle satellite cells (MuSCs) from hindlimb muscles.

Figure S7

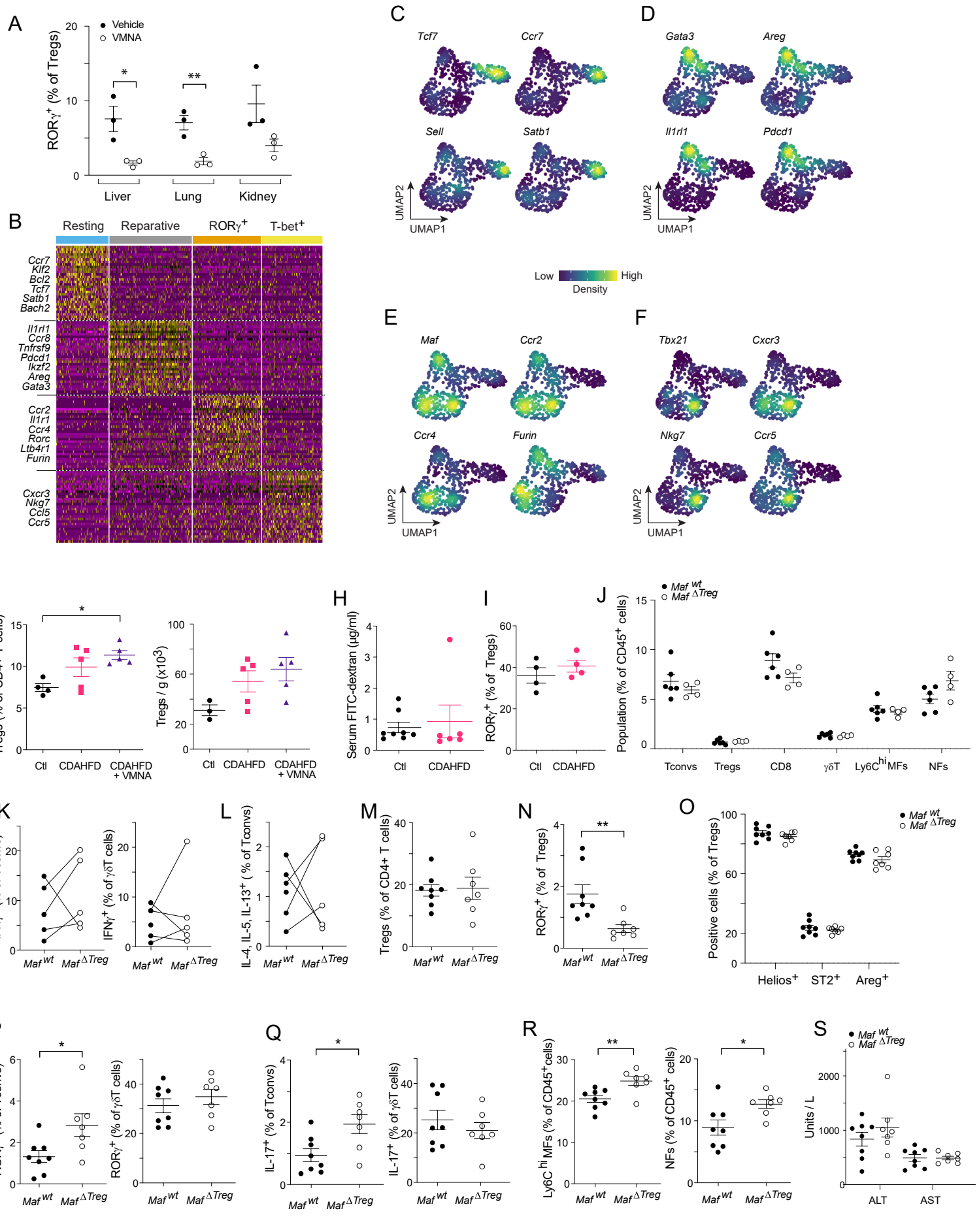
A
Vehicle
VMNA
RORγ+ (% of Tregs)
Liver
Lung
Kidney
B
Resting
Reparative
RORγ+
T-bet+
Ccr7
Klf2
Bcl2
Tcf7
Satb1
Bach2
Il1rl1
Ccr8
Tnfrsf9
Pdcd1
Ikzf2
Areg
Gata3
Ccr2
Il1r1
Ccr4
Rorc
Ltb4r1
Furin
Cxcr3
Nkg7
Ccl5
Ccr5
C
Tcf7
Ccr7
Sell
Satb1
UMAP1
UMAP2
D
Gata3
Areg
Il1rl1
Pdcd1
Low
High
Density
E
Maf
Ccr2
Ccr4
Furin
F
Tbx21
Cxcr3
Nkg7
Ccr5
G
Tregs (% of CD4+ T cells)
Tregs / g (x10^3)
Ctl
CDAHFD
CDAHFD + VMNA
H
Serum FITC-dextran (μg/ml)
I
RORγ+ (% of Tregs)
J
Maf wt
Maf ΔTreg
Population (% of CD45+ cells)
Tconvs
Tregs
CD8
γδT
Ly6Chi MFs
NFs
K
IFNγ+ (% of Tconvs)
IFNγ+ (% of γδT cells)
L
IL-4, IL-5, IL-13+ (% of Tconvs)
M
Tregs (% of CD4+ T cells)
N
RORγ+ (% of Tregs)
O
Positive cells (% of Tregs)
Helios+
ST2+
Areg+
P
RORγ+ (% of Tconvs)
RORγ+ (% of γδT cells)
Q
IL-17+ (% of Tconvs)
IL-17+ (% of γδT cells)
R
Ly6Chi MFs (% of CD45+ cells)
NFs (% of CD45+ cells)
S
Units / L
ALT
AST

Figure S7 (Related to Figure 7): Regulation of inflammation in extra-gut tissues by microbiota-dependent RORγ$^+$ Treg cells

(A) Flow-cytometric quantification of RORγ$^+$ Treg cells in diverse tissues of SPF mice that were treated or not with the Abx cocktail, VMNA. (B-F) scRNA-seq of cardiac muscle Treg cells after myocardial infarction (taken from Xia et al.). B) Heatmap of the top 30 differentially expressed genes in each cluster. C) Resting, D) reparative, E) RORγ$^+$ and F) T-bet$^+$ Treg clusters' expression of key marker genes shown as density plots. (G) Flow-cytometric quantification of liver Treg cells after one week of feeding with control diet (Ctl) or with choline-deficient, L-amino acid-defined, high-fat diet (CDAHFD) ± VMNA. (H, I) B6 mice were fed with Ctl or CDAHFD for one week. H) Intestinal permeability measured by FITC-dextran serum concentrations, and I) flow-cytometric quantification of colon RORγ$^+$ Treg cells. (J) Flow-cytometric quantification of the indicated liver immunocyte compartments at steady-state in *Maf*$^{\Delta Treg}$ and *Maf*^{wt} littermates. (K, L) *Maf*$^{\Delta Treg}$ and *Maf*^{wt} littermates were fed with CDAHFD for one week. Quantification of K) IFNγ, and L) IL-4+IL-5+IL-13 expression following PMA+ionomycin stimulation of the indicated effector T cell population. (M-S) *Maf*$^{\Delta Treg}$ and *Maf*^{wt} littermates were fed with CDAHFD for 8 weeks. Flow-cytometric quantification of liver M) total Treg cells, N) RORγ$^+$ Treg cells, O) Helios$^+$, ST2$^+$, Areg$^+$ Treg cells, P) RORγ$^+$ Tconv (left) and γδT cells (right), Q) IL-17A production by Tconv and γδT cells, and R) fraction of Ly6C^{hi} MFs (left) and NFs (right). S) Plasma concentrations of alanine transaminase (ALT) and aspartate aminotransferase (AST). One-way ANOVA (G), otherwise an unpaired t-test.

Table S1 (Related to Figures 1, 2, 4 and 5): Summary and quality-control metrics of scRNA-seq datasets

scRNA-seq

Dataset	*Genotype / treatment*	*Sorting strategy*	*Hashtaged*	*Total cells passing QC*	*Minimum genes / cell threshold*	*Maximum UMI / cell threshold*	*Median genes / cell*	*Median UMI / cell*
Muscle Tregs d3 post CTX	*Foxp3*^{GFP}	TCRb^{+} CD4^{+} Foxp3^{GFP+}	No	2020	500	4000	756	1252.5
Muscle Tregs d3 post CTX	*Foxp3*^{GFP} + Vehicle	TCRb^{+} CD4^{+} Foxp3^{GFP+}	Yes	380	1000	7000	1711.5	4081.5
Muscle Tregs d3 post CTX	*Foxp3*^{GFP} + VMNA	TCRb^{+} CD4^{+} Foxp3^{GFP+}	Yes	389	1000	7000	1713	4152
Muscle Tregs d3 post CTX	*Foxp3*$^{YFP\text{-}Cre}$ *x Maf*$^{wt/wt}$	TCRb^{+} CD4^{+} Foxp3^{YFP+}	Yes	228	1000	7000	1675.5	4166.5
Muscle Tregs d3 post CTX	*Foxp3*$^{YFP\text{-}Cre}$ *x Maf*$^{fl/fl}$	TCRb+ CD4+ Foxp3^{YFP+}	Yes	324	1000	7000	1781.5	4670.5

scRNA-seq/sc*Tcr*- seq

Dataset	*Genotype / treatment*	*Sorting strategy*	*Hashtaged*	*Total cells passing QC*	*Minimum genes / cell threshold*	*Maximum UMI / cell threshold*	*Median genes / cell*	*Median UMI / cell*
Muscle Treg d3 post CTX_batch 1	*Foxp3*^{GFP}	TCRb^{+} CD4^{+}	Yes	504	750	10000	1450	3380
Colon Treg d3 post CTX_batch 1	*Foxp3*^{GFP}	TCRb^{+} CD4^{+} Foxp3^{GFP+}	Yes	2281	750	10000	1406	3275
Muscle Treg D3 post CTX_batch 2	*Foxp3*^{GFP}	TCRb^{+} CD4^{+}	Yes	1025	500	5000	899	1692